Tellus (1995), 47B, 35–52
Printed in Belgium – all rights reserved

TELLUS
ISSN 0280–6509

A synthesis inversion of the concentration and $\delta^{13}C$ of atmospheric CO_2

By I. G. ENTING*, C. M. TRUDINGER and R. J. FRANCEY, *CSIRO, Division of Atmospheric Research Private Bag 1, Mordialloc Victoria 3195, Australia*

(Manuscript received 22 November 1993; in final form 29 August 1994)

ABSTRACT

A synthesis inversion technique is used to estimate CO_2 fluxes to and from the atmosphere. Concentrations calculated by the GISS atmospheric tracer transport model are fitted to observations of CO_2 and $^{13}CO_2$. The procedure uses the uncertainty in the data to derive measures of uncertainty for the estimated sources, thus allowing a comparison of the relative importance of various data items in reducing these uncertainties. We analysed two periods. The first, 1986–1987, was intended to be representative of these and earlier years. The CO_2 data appear generally representative but the inversion produces some features that may reflect El Niño conditions. The second period was 1989–1990 which had anomalous behaviour in $\delta^{13}C$. The attempt to analyse 1989–1990 was somewhat unsatisfactory, apparently because the assumption of a quasi-steady state, required by our analysis, was not satisfied sufficiently well. The main result is that global totals of oceanic versus biotic exchange are constrained primarily by the global trends of CO_2 and $^{13}CO_2$. The transport model constrains the regional sources and sinks but these constraints make only a small contribution to reducing the uncertainty in the global budget. We find that within the range of ≈ 1.2 Gt C y^{-1} our unconstrained estimates of air-sea flux are very sensitive to the choice of data that are fitted. This confirms the appropriateness of our formal error estimates based on a priori statistics.

1. Introduction

In spite of a large amount of research, the atmospheric budgets of greenhouse gases are still subject to considerable uncertainty. For carbon dioxide (CO_2) and methane (CH_4) most recent estimates of atmospheric budgets have used atmospheric transport modelling to interpret the space-time distributions of concentrations in terms of the space-time distributions of sources and sinks (Keeling et al., 1989b; Tans et al., 1990a; Sarmiento and Sundquist, 1992; Fung et al., 1991). The principle is that, to the extent that the spatial distribution of sources and sinks can be deduced from observations, the location will act as a constraint on the possible processes (Pearman and Hyson, 1986). The potential advantage of this technique is that it gives a short-term "snap-shot" of the atmospheric carbon budget, unlike other approaches such as ocean modelling that give longer-term averages.

However, the determination of surface sources and sinks from observations of surface concentrations is a poorly-determined inverse problem (Newsam and Enting, 1988; Enting and Newsam, 1990; Enting, 1993). As such, direct estimates of sources are subject to arbitrarily large errors arising from errors in any or all of the observations, the transport model or the inversion technique. In general, meaningful estimates can only be obtained in the context of a set of prior constraints. The most common form of such constraints is in terms of spatial (and temporal) smoothness.

Most inversions using three-dimensional transport models have been based on some sort of "synthesis" approach (Keeling et al., 1989b; Tans et al., 1990a; Fung et al., 1991). The method involves seeking a linear combination of source/

* Corresponding author.

sink processes such that the corresponding linear combination of their calculated responses matches the observational data. In synthesis calculations the solutions are stabilised by the assumptions about the spatial distributions of the source components.

We present a synthesis inversion that uses the trends and spatial and seasonal distributions of CO_2 and $^{13}CO_2$ to obtain estimates of the various contributions to the atmospheric CO_2 budget. As in our earlier global carbon cycle modelling (Enting and Pearman, 1987) we use a Bayesian analysis. Specifically, the estimation is stabilised by introducing additional contraints in the form of independent prior estimates of the source strengths. An account of many of the technical details is given by Enting et al. (1993). A particularly important aspect of our analysis is that we are able to determine the extent to which uncertainties in the observational data lead to uncertainties in the estimated sources. (We have not, however, been able to quantify the range of uncertainty associated with errors in the atmospheric transport model).

In discussing atmospheric budgets, we need to distinguish between three distinct quantities.

CO_2 fluxes. Our use of CO_2 data means that we are obtaining estimates of CO_2 fluxes.

Carbon fluxes. The carbon flux differs from the CO_2 flux because of the release of other carbon compounds into the atmosphere. The majority of such carbon is ultimately oxidised to CO_2 via carbon monoxide (CO). On a global basis, this implies that the total net CO_2 input to the atmosphere (including production from CO) equals the total net carbon flux, but on a regional basis the two quantities differ (Enting and Mansbridge, 1991). Their estimated 0.86 Gt C y^{-1} CO_2 source from CO oxidation in the free atmosphere represents the balance of estimated sources of 0.3 Gt C y^{-1} from fossil carbon, 0.56 Gt C y^{-1} as CO from biotic sources, 0.05 Gt C y^{-1} as CH_4 from wetlands and 0.12 Gt C y^{-1} from other CH_4 sources, less a sink of 0.17 Gt C y^{-1} due to surface oxidation of CO.

Carbon storage. The other distinction to consider is that the rate of carbon storage in a reservoir will not be equal to the net carbon flux to that reservoir from the atmosphere if other inter-reservoir transfers occur. In particular, transfer of carbon from the terrestrial biota to the oceans via rivers (Sarmiento and Sundquist, 1992) implies a difference of about 0.6 Gt C y^{-1} between air-sea carbon flux and ocean carbon storage.

In relating these different quantities, we advocate the use of the term *conversion* from one type of quantity to another rather than the term *correction* which has often been used. It is not that any of the three quantities is "wrong" (and thus in need of correction) but rather that three different quantities are involved.

Given our sign convention of taking inputs to the atmosphere as positive, 0.86 Gt C y^{-1} CO oxidation source of CO_2 corresponds to taking a fossil CO_2 source 0.3 Gt C y^{-1} lower than the fossil carbon source. Similarly the (negative) flux from biotic CO_2 uptake is 0.56 Gt C y^{-1} more negative than the biotic carbon uptake flux. The river carbon term implies that the biotic carbon uptake flux is in turn 0.6 Gt C y^{-1} more negative than the biotic carbon storage rate.

The reverse operation is conversion of the estimated CO_2 fluxes obtained from the inversion into estimates of carbon storage. This involves taking the estimated net CO_2 flux from the terrestrial biota, adding 0.6 Gt C y^{-1} to account for carbon that enters the biota from the atmosphere but which is transfered to the oceans via rivers rather than being stored and adding a further 0.56 Gt C y^{-1} to account for carbon that enters the biota as CO_2 but which leaves in the form of CO or some CO precursor. (The 0.56 may be replaced by a modified value based on the CO source).

These conversion terms need to be taken into account both in the interpretation of results from inversion calculations and in the determination of prior fluxes for the Bayesian estimation.

The outline of the remainder of this paper is as follows: Section 2 describes the inversion technique that we adopted, with particular emphasis on the estimation of uncertainties. Section 3 describes the way in which the source processes are divided into distinct components for use in the synthesis analysis. Section 4 describes the observational data used in the studies. The results of the inversions are presented in Section 5. Section 6 discusses further aspects of the calculations of uncertainties. Section 7 concludes with a discussion of the implications of our results for the global carbon cycle and

reviews the areas in which a refinement of the present studies seem possible and desirable. Appendix A defines the units used and Appendix B lists the notation.

2. Formalism

2.1. General

The synthesis process seeks to estimate the strengths, σ_μ, of N source/sink processes by comparing M observed concentrations, c_j, (with standard deviations, u_j) to responses calculated using an atmospheric transport model. If the model response for observation j to a source μ of unit strength is $T_{j\mu}$, then the fit is made on the assumption that

$$c_j = \sum T_{j\mu}\sigma_\mu + \text{observational noise.} \tag{1}$$

In the Bayesian formalism, the fit is constrained to take account of prior estimates, $s_\mu \pm v_\mu$, of the source strengths. Subsequent to the study by Enting et al. (1993) we have added the option of applying L additional constraints (of the form $\sum_\mu q_{\beta\mu}\sigma_\mu = t_\beta \pm r_\beta$) to sums over groups of source components.

We consider the least-squares Bayesian inversion obtained by minimising

$$\Theta = \sum_{j=1}^{M}\left(c_j - \sum_{\mu=1}^{N'} T_{j\mu}\sigma_\mu\right)^2 \Big/ u_j^2 + \sum_{\mu=1}^{N}(\sigma_\mu - s_\mu)^2/v_\mu^2 + \sum_{\beta=1}^{L}\left(\sum_\mu q_{\beta\mu}\sigma_\mu - t_\beta\right)^2 \Big/ r_\beta^2. \tag{2}$$

Taking $N' > N$ allows for some additional "pseudo-sources" representing the mean levels of CO_2, $\delta^{13}C$ of CO_2. We exclude these pseudo-sources from the fit to the prior estimates.

The minimisation leads to a set of linear equations that are solved using a modified version of routine SVDFIT (and the routines which it calls) from Press et al. (1986). This produces estimates, $\hat{\sigma}_\mu$, of the source strengths. The routine SVDVAR is used to calculate the covariance matrix $V_{\mu\eta}$ for these estimates.

We also include the capability of calculating the residuals to eq. (1), and the ability to look at the covariances of linear combinations of the source components such as global sums of biotic or ocean exchange.

The formalism above requires a discretisation in the time domain. We have assumed a quasi-steady state so that we can discretise in terms of a global trend plus annual cycles represented as Fourier series. Alternative discretisations of time are discussed by Enting (1995).

2.2. Isotopes

For $^{13}CO_2$ the definition of the "δ" notation is

$$\delta^{13}C = [\,{}^{13}C{:}{}^{12}C_{\text{sample}}/{}^{13}C{:}{}^{12}C_{\text{standard}} - 1\,] \times 1000 \tag{3}$$

in units of per mil (denoted $^{o}/_{oo}$).

The ^{13}C anomaly used in the calculations is

$$X = ([\,{}^{13}C]/R_{\text{ref}} - [\,C]) \times 1000. \tag{4a}$$

where R_{ref} is a reference $^{13}C{:}(C^{12} + {}^{13}C)$ ratio. X acts as a conservative tracer, since it is a linear combination of two conserved tracers. We choose R_{ref} to correspond to a $\delta^{13}C$ of -8, close to the observed atmospheric mean. With this definition, we have, to a good approximation (see Enting et al., 1993):

$$X = (\delta^{13}C + 8)[\,C]. \tag{4b}$$

The reason for this choice of offset in defining X can be seen when we consider the trend in X. We have:

$$\frac{d}{dt}X = (\delta^{13}C + 8)\frac{d}{dt}[\,C] + [\,C]\frac{d}{dt}\delta^{13}C. \tag{5}$$

By choosing R_{ref} so that the factor $(\delta^{13}C + 8)$ is close to zero, the uncertainty in the trend in X is almost entirely due to the uncertainty in $d/dt(\delta^{13}C)$, independent of uncertainties in the corresponding CO_2 data. Seasonal and spatial variations in X are similarly independent of errors in CO_2.

3. Components

3.1. Requirements

The synthesis analysis involves three sets of quantities: (i): a set of source components that

are assumed to characterise the system. For each component the space and time distributions and assumed isotopic composition are taken as known. These source strengths are the quantities that are to be estimated. It is assumed that we have prior estimates of the form $s_\mu \pm v_\mu$. Since these are poorly known (which is the reason for performing the synthesis calculation) we round all values s_μ, v_μ to the nearest 0.1 Gt C y^{-1}. (ii): a set of observational data to be fitted; and (iii): a set of calculated model responses that specify each source component's normalised contribution to the calculated value of each item of observational data.

The assumption underlying the synthesis approach is that the space-time distribution of each of the source components is known apart from an overall "source-strength" factor. There is a risk that this assumption can "overspecify" the problem. For ocean inverse problems, Wunsch and Minster (1982) recommend that, for a realistic treatment of uncertainties, an underdetermined formulation of the problem is required. The principle is that in an ill-conditioned problem the data will specify only a small number of degrees of freedom in the solution but that the problem should be formulated so that *the resolution is determined by the data* and not by some arbitrary initial prescription of a restricted solution space. For this reason we have used many more components (54, including 20 for purely isotopic effects) than the 9 (see Heimann and Keeling, 1989, p. 248) that were used by Keeling et al. (1989b).

The calculations of the concentrations produced by each of the source distributions were performed using the GISS tracer transport model described by Russell and Lerner (1981) and Fung et al. (1983). We used the "low-resolution" version with an $8° \times 10°$ grid. A year of 4-hourly-averaged winds and monthly-averaged convection generated by the GISS GCM (running at $4° \times 5°$ resolution) was used to specify the model transport. The model also includes a "diffusive" transport, as described by Prather et al. (1987). All source components were normalised to 1 Gt C y^{-1} per year annual mean release, except for seasonal sources which were normalised to 1 Gt C y^{-1} annual mean NPP.

In the analysis presented here, we assume a quasi-steady state with sources and concentrations that are periodic except for a globally uniform trend. For periodic sources a steady-state (i.e., an annually periodic cycle plus a globally uniform trend) is achieved after 3 years. Therefore the detrended series for year 4 from each site are fitted with Fourier components to define the responses for the various space-time distributions of sources.

3.2. *Fossil*

The space-time distribution of the fossil source is based on estimates of the global distribution of CO_2 emissions due to fossil-fuel burning, and cement production, for 1980 (Marland et al., 1985). Seasonal variation is incorporated into the source by distributing the total annual release throughout the year using monthly fossil-fuel CO_2 emissions for 1982 from Rotty (1987). Enting et al. (1993) used a $\delta^{13}C$ of $-27‰$ based on the data from Tans (1981). For the present calculations we use $-28.2‰$ based on estimates by Andres et al. (1995).

The prior estimates of fossil carbon sources are taken from CDIAC (1991). The standard deviations of these prior estimates are taken as 5% of the total. Since the inversion is estimating CO_2 fluxes, we reduce the prior estimates by 0.3 Gt C y^{-1} to take account of CO emissions from incomplete combustion, giving 5.3 ± 0.3 for 1986–1987 and 5.7 ± 0.3 for 1989–1990. (A description of the role of carbon monoxide in relating the carbon and CO_2 budgets of the atmosphere is given by Enting and Mansbridge, 1991).

3.3. *Oceans*

The ocean is divided into 12 regions, each of which is assumed to be uniform. The characteristics are summarised in Table 1. (The initial case considered by Enting et al. (1993) combined the 4 equatorial regions.) Sources in each of the ocean regions are modelled separately. No seasonal variations in the ocean fluxes are considered in this study.

The net CO_2 flux is the difference between two gross fluxes: $\Phi_{am} = a\kappa p_a$ and $\Phi_{ma} = a\kappa p_m$ where a is the area of the ocean region, κ is a gas-exchange coefficient (not necessarily the same for all regions) and p_a and p_m are the CO_2 partial pressures in the atmosphere and mixed layer respectively. Thus the net flux is

$$S_N = \Phi_{ma} - \Phi_{am} = a\kappa \, \Delta p_{CO_2}. \qquad (6)$$

Table 1. *Prior estimates of CO_2 fluxes (with uncertainties) from ocean regions*

Region	Net flux (Gt C y^{-1})	Disequilibrium effect ($^o/_{oo}$ Gt C y^{-1})
>48° N:		
Atlantic	-0.2 ± 0.5	$-0.94 \times (2.7 \pm 1.4)$
Pacific	0.2 ± 0.5	$-1.08 \times (2.5 \pm 1.3)$
16° N to 48° N:		
Atlantic	-0.3 ± 1.0	$0.67 \times (5.1 \pm 2.6)$
Pacific	-0.3 ± 1.0	$0.75 \times (8.7 \pm 4.4)$
16° S to 16° N:		
west Pacific	0.3 ± 1.0	$0.63 \times (4.0 \pm 4.0)$
east Pacific	0.6 ± 1.0	$1.63 \times (4.0 \pm 4.0)$
Atlantic	0.3 ± 1.0	$1.39 \times (4.0 \pm 4.0)$
Indian	0.3 ± 1.0	$1.42 \times (4.0 \pm 4.0)$
48° S to 16° S:		
Atlantic	-0.5 ± 1.0	$0.43 \times (4.0 \pm 2.0)$
Pacific	-1.0 ± 1.5	$0.74 \times (8.4 \pm 4.2)$
Indian	-0.7 ± 1.0	$0.46 \times (5.7 \pm 2.9)$
<48° S:		
southern	-0.2 ± 1.0	$-1.50 \times (22.3 \pm 11.0)$

The effect of isotopic disequilibrium on the ^{13}C anomaly budget is calculated by treating the $\delta^{13}C$ difference (the initial factor in the last column) as precisely known and formally attributing all uncertainties to the gross flux (the term in brackets).

The determination of the annual mean net flux for large ocean regions using direct measurements is limited by (a) uncertainties (of a factor of 2) in the gas-exchange coefficient and (b) the limited spatial and temporal coverage of the ocean p_{CO_2} data set.

The $^{13}CO_2$ flux is given by

$$S^* = \alpha_{ma} R_m \Phi_{ma} - \alpha_{am} R_a \Phi_{am}. \tag{7a}$$

The ocean contribution to the isotopic anomaly X is

$$\begin{aligned} S_X &= (S^*/R_{ref} - S_N) \times 1000 \\ &= [\alpha_{am} R_a / R_{ref} - 1][\Phi_{ma} - \Phi_{am}] \times 1000 \\ &+ \Phi_{ma}[\alpha_{ma} R_m - \alpha_{am} R_a] \times 1000/R_{ref}. \end{aligned} \tag{7b}$$

Thus, the isotopic response splits into a component proportional to the net CO_2 flux S_N and a component proportional to the gross sea-to-air flux Φ_{ma}. This second component is driven by the degree of isotopic disequilibrium $\alpha_{ma} R_m - \alpha_{am} R_a$ between the atmosphere and the mixed layer and affects only the isotopic distribution. It is expressed as:

$$\begin{aligned} S_G &= \Phi_{ma}[\alpha_{ma} R_m - \alpha_{am} R_a] \times 1000/R_{ref} \\ &= \Phi_{ma} \alpha_{am} \frac{R_a}{R_{ref}} \left[\frac{\alpha_{ma}}{\alpha_{am}} \frac{R_m}{R_a} - 1 \right] \times 1000. \end{aligned} \tag{8}$$

Thus, estimation of this term requires: (i) the gross sea-to-air flux, Φ_{ma}; (ii) data for the isotopic composition of atmospheric and ocean surface carbon (R_a and R_m); (iii) estimates of the fractionation factors, α_{am} and α_{ma} for which temperature dependence is important. Each of these factors involves significant uncertainties, but for the purposes of the inversion, only the combined uncertainty in the product need be considered (Enting et al., 1993). We calculate the appropriate prior uncertainty for the product, but perform the calculations as if all this uncertainty was associated with the fluxes Φ_{ma}, as indicated in the final column of Table 1. These estimates for the isotopic disequilibria are based on the data presented by Tans et al. (1993), converted to our grid using area-weighted averages.

In summary, each ocean region is represented by two source components: a net flux term affecting both total CO_2 and the ^{13}C anomaly and a gross-flux term affecting only the ^{13}C anomaly. In each region, we assume that the spatial distribution of gross and net fluxes is the same. Therefore we use the same calculated response distribution for the gross flux and net flux components.

3.4. *Biotic fluxes*

The biotic influences on atmospheric carbon are represented in terms of 4 processes, each of which is subdivided regionally. The effects of these processes are calculated using combinations of three sets of space-time distributions of sources, again subdivided regionally. The first two sets of space-time distributions are *release* and *uptake* which have the same spatial patterns but which differ in the time dependence. These distributions are divided into eight regions as indicated in Table 2. The third set of space-time distributions are for *land-use*, divided into 4 regions as indicated in Table 3. The processes that we consider are *land-use* which uses the 4 *land-use* distributions, *seasonal* which uses the 8 differences between *uptake* and *release* distributions, *unbalanced uptake* processes which use the eight *uptake* distributions,

Table 2. *Prior estimates of CO_2 fluxes (with uncertainties) for "natural" responses of terrestrial systems*

Type	Uptake (Gt C y^{-1})	Disequilibrium ($^{o}/_{oo}$ Gt C y^{-1})	Seasonal (Gt C y^{-1})
tropical forest, America	0.0 ± 1.5	$0.3 \times (18.6 \pm 18.6)$	8.5 ± 2.0
tropical forest, Africa	0.0 ± 1.5	$0.3 \times (6.1 \pm 6.1)$	2.8 ± 2.0
tropical forest, Asia	0.0 ± 1.5	$0.3 \times (14.7 \pm 14.7)$	6.7 ± 2.0
temperate evergreen	0.0 ± 1.5	$0.3 \times (3.1 \pm 3.1)$	1.4 ± 2.0
temperate deciduous	0.0 ± 1.5	$0.3 \times (16.0 \pm 16.0)$	7.3 ± 2.0
boreal forest	0.0 ± 1.5	$0.3 \times (7.7 \pm 7.7)$	3.5 ± 2.0
grassland	0.0 ± 1.5	$0.3 \times (20.6 \pm 20.6)$	9.4 ± 2.0
other	0.0 ± 1.5	$0.3 \times (13.2 \pm 13.2)$	6.0 ± 2.0

The seasonal component is expressed in terms of NPP, using the time variations obtained by Azevedo (1982). The isotopic disequilibrium is treated in the same way as in Table 1.

and *isotopic disequilibrium* which uses the eight *release* distributions.

These *land-use*, *seasonal* and *unbalanced uptake* processes affect both total CO_2 and ^{13}C for which we assume a $\delta^{13}C$ of $-25^{o}/_{oo}$. An extra contribution to only the atmospheric $^{13}CO_2$ budget arises from an *isotopic disequilibrium* process as described below. Tables 2 and 3 list the prior estimates of the fluxes for the biotic components.

The spatial distribution of net primary production (NPP) is used to determine the uptake and release space-time distributions within the specified regions. The NPP distribution is calculated using source estimates from Pearman and Hyson (1986) for 10 different vegetation types, combined with vegetation maps at $1^{\circ} \times 1^{\circ}$ from Matthews (1985). The seasonal variations of uptake and release are taken to be functions of latitude and are based on the curves used by Fung et al. (1983) which were taken from the thesis of Azevedo (1982) (see Fig. 3 of Enting et al., 1993 for details). For northern latitudes greater than 70°, we assume that the uptake is concentrated over June and July and the release over April through September. The use of specified functions of time means that, for each latitude zone, the strength of the seasonal cycle is uniquely related to NPP. Since the annual means of these seasonal fluxes are zero, we use these NPP values to report cycle strengths.

Table 3. *Prior estimates of CO_2 fluxes (with uncertainties) for fossil source (excluding CO) (Andres et al., 1994; CDIAC, 1991), CO (Enting and Mansbridge, 1991) and Land-use (Houghton et al., 1987)*

Source	Prior (Gt C y^{-1})
fossil (86–87)	5.3 ± 0.3
fossil (89–90)	5.7 ± 0.3
CO	0.9 ± 0.2
Land-use:	
tropical America	0.6 ± 0.5
tropical Africa	0.4 ± 0.5
tropical Asia	0.6 ± 0.5
other	0.2 ± 0.3

Land-use. The source of carbon due to land-use changes (the net effect of clearing of forests for agriculture, forest regrowth etc.) is discussed in Houghton et al. (1987). They gave the regional distribution an estimated 1.791 Gt C y^{-1} source for 1980. We construct the four *land-use* distributions by distributing these totals within each region in proportion to the spatial distribution of net primary productivity described above, but redefine the seasonality. A peak of 20% in the source is imposed during the 3 driest months of the year in the tropics to reflect increased biomass burning in the dry season.

Uptake. This component represents those biotic sinks of CO_2 that are not balanced by natural CO_2 sources at the point of uptake. Such uptakes occur when there is either storage of carbon in the ecosystem or a transport of carbon away from the system in a form other than atmospheric CO_2. The storage term is generally equated to the effect of stimulated plant growth due to increased levels of atmospheric CO_2. However, if we assume that the "land-use" term

represents *all* the net CO_2 flux arising from change in land-use then, for a complete description, the "uptake" term must include all other changes in terrestrial biomass. This will include both additional uptake from the effects of nutrient changes and reduced uptake resulting from toxification. Enting et al. (1993) used an aggregated representation of the uptake process with a prior estimate of -2.8 ± 1.0 Gt C y^{-1} after taking into account the roles of CO and river carbon. In our eight-region disaggregation presented here we have used prior estimates of 0 with very conservative estimates of ± 1.5 Gt C y^{-1} for each of the prior uncertainties.

Isotopic disequilibrium. The $\delta^{13}C$ of the terrestrial biota is changing due to the changing $\delta^{13}C$ of the atmospheric carbon taken up in photosynthesis. However this biotic change will lag behind the atmospheric change and so the $\delta^{13}C$ of carbon released from the biota will be higher than that of carbon taken up. Therefore there is a contribution to the atmospheric ^{13}C anomaly budget from isotopic disequilibrium of the terrestrial biota. Enting et al. (1993) used the biotic model of Emanuel et al. (1981) combined with the ice-core $\delta^{13}C$ data from Friedli et al. (1986) to estimate this disequilibrium contribution as $26.5‰$ Gt C y^{-1}. For our standard cases we have taken the degree of disequilibrium from the globally aggregated calculation and distributed it in proportion to NPP. Possible changes in global fractionation due to photosynthesis are expected to be small, at least when averaged over several years, and are not considered here.

3.5. *Carbon monoxide*

The significance of CO in CO_2 inversions was pointed out by Enting and Newsam (1990) and quantified by Enting and Mansbridge (1991). The CO_2 source from CO is taken as uniform in time and longitude and vertically uniform through the troposphere, with the latitudinal distribution from Enting and Mansbridge (1991).

We take the $\delta^{13}C$ of the CO_2 produced as being characteristic of biotic and fossil carbon, on the basis that in a quasi-steady-state situation (i.e., time-scales longer than the CO lifetime of weeks to months), the isotopic compositions of the production and loss fluxes for atmospheric CO must be the same.

The only component of the CO budget required for the inversion is the net rate of CO_2 production from CO oxidation. We use the value 0.86 Gt C y^{-1} (Enting and Mansbridge, 1991), rounded to the nearest 0.1 Gt C y^{-1} as for other prior estimates. The standard deviation of 0.2 Gt C y^{-1} reflects the proportional uncertainty in the average OH concentration (and hence the CO sink) based on the study by Prinn et al. (1987).

4. Data

The synthesis analyses presented in this paper are intended to give estimates of the atmospheric carbon budget representative of the periods 1986–1987 and 1989–1990. As noted above, we assume a quasi-steady state with periodic sources and concentrations that are periodic except for a globally uniform trend. Therefore for CO_2 and $\delta^{13}C$ the relevant observational data items are (i) the global trends; (ii) the Fourier components of the seasonal cycle; (iii) the mean (decycled) values at individual sites at some reference time. The nature of the fit means that we do not need a complete set of such data (unlike the surface mass balance inversions of Enting and Mansbridge, 1989, 1991; Tans et al., 1989). However, for each data item we require the value, c_j, and an estimate of the uncertainty, u_j. The expression of ^{13}C data as an isotopic anomaly, X, means that when using ^{13}C data we require the corresponding CO_2 data.

Our main source of CO_2 data is the set of mean concentrations from the NOAA flask sampling network. We use averages of the 1986 and 1987 annual means, as tabulated in GMCC (1988) and averages of the 1989 and 1990 annual means, as tabulated in CMDL (1992). The values for land stations are listed in Table 4. For 1989–1990 we also include data from the NOAA ship-based sampling program. The range of uncertainty is taken as 0.3 ppmv for each data point. This range is based on the work of Tans et al. (1990b) who used a simulation approach to explore the statistical characteristics of the NOAA flask sampling procedures. The Fourier components of the seasonal cycles were obtained by regression fits to NOAA data tabulated in CDIAC (1991). We also use global mean growth rates as described in Sections 5a and 5b below.

The atmospheric $\delta^{13}C$ data come from the CSIRO global flask network (see Francey and Goodman, 1986, 1988; Francey et al., 1990;

Table 4. *CO_2 data in ppmv: two-year means for 1986-1987 and 1989-1990, and 12-month Fourier component of the seasonal cycle (NOAA data from CDIAC, 1991); we also use the CO_2 growth rates listed in Subsections 5a, b*

Code	Site	Lat	86–87	89–90	cos	sin
ALT	Alert	82.5	348.75	355.30	2.12	6.00
MBC	Mould Bay	76.2	349.20	355.75	2.16	6.18
BRW	Barrow, Alaska	71.3	349.05	355.50	2.53	5.94
STM	Ocean Station M	66.0	348.00	354.40	2.56	5.72
CBA	Cold Bay, Alaska	55.2	348.90	354.85	3.13	5.73
SHM	Shemya Is.	52.8	349.45	354.75	4.06	5.99
CMO	Cape Meares	45.0	349.30	354.90	2.25	3.84
AZR	Azores	38.8	348.70	352.10	1.44	4.15
MID	Midway	28.2	348.65	354.65	0.00	3.60
KEY	Key Biscayne	25.7	348.55	355.35	−0.04	3.27
KUM	Cape Kumukahi	19.5	347.50	353.60	−0.45	3.39
AVI	Virgin Is.	17.8	347.30	—	−0.38	3.40
GMI	Guam	13.4	348.40	353.85	−1.02	2.75
RPB	Barbados	13.2	—	353.80	—	—
CHR	Christmas Is.	2.0	347.40	353.80	−0.49	1.39
SEY	Seychelles	−4.7	347.50	352.75	0.59	1.08
ASC	Ascension Is.	−7.9	346.95	352.25	−0.37	−0.51
SMO	Samoa	−14.3	346.25	352.15	0.02	0.26
CGO	Cape Grim, Tas	−40.7	345.55	350.90	−0.10	−0.48
PSA	Palmer Station	−64.9	345.85	351.40	−0.17	−0.68
SPO	South Pole	−90.0	345.70	351.20	0.00	−0.59

Francey et al., 1995). It should be pointed out that the inter-annual variability in the CSIRO data set over the 1982 to 1988 period is 3–5 times smaller than that reported by Keeling et al. (1989a). The reasons for this discrepancy have not yet been uncovered. We use the global trend based on our long $\delta^{13}C$ record from Cape Grim.

The values used in the inversions are listed in Table 5. The Mauna Loa data are included for completeness but were not used in the inversions

Table 5. *^{13}C data: two-year means for 1986-1987 and 1989-1990*

	1986–1987		1989–1990	
Site code	$\delta^{13}C$ (‰)	X (‰ ppmv)	$\delta^{13}C$ (‰)	X (‰ ppmv)
ALT	—	—	-8.0175 ± 0.404	-6.22 ± 143.80
BRW	-7.899 ± 0.027	35.25 ± 10.1	-8.0415 ± 0.099	-14.75 ± 35.05
CPU	—	—	-7.895 ± 0.118	37.254 ± 41.87
MLO	-7.686 ± 0.017	109.08 ± 5.9	-7.7865 ± 0.053	75.46 ± 18.69
SMO	-7.638 ± 0.013	125.31 ± 4.5	—	—
CGO	-7.644 ± 0.010	123.01 ± 3.5	-7.7335 ± 0.028	93.51 ± 9.81
SPO	-7.661 ± 0.010	117.19 ± 3.5	-7.7435 ± 0.031	90.08 ± 10.86
	(‰ y^{-1})	(‰ ppmv y^{-1})	(‰ y^{-1})	(‰ ppmv y^{-1})
trend	-0.030 ± 0.005	-10.1 ± 1.7	0.000 ± 0.005	0.19 ± 1.7

The Cheeka Peak (CPU) data were supplied by P. D. Quay. Abbreviations are as for Table 4. The Mauna Loa (MLO) data are included for completeness but were excluded from the inversions because the response functions only apply for surface sites.

as the response functions only apply to surface sites. Enting et al. (1993) explored inversions in which the Mauna Loa data were fitted with surface ^{13}C values. The South Pole value for 1986–1987 differs slightly from that quoted and used by Enting et al. (1993) due to a minor error in their work. Seasonal cycles of $\delta^{13}C$ were not used, since our model has an incomplete treatment of seasonal fluxes. The work of Pearman and Hyson (1986) suggests that seasonal ^{13}C data will provide useful constraints on seasonal fluxes from the oceans.

5. Results

5.1. The period 1986–1987

Table 6 shows the results of 3 inversion estimates for 1986–1987. The first two of these use the CO_2 growth rate of 1.80 ± 0.15 ppmv y^{-1} as used by Enting et al. (1993). This was obtained from running mean gradients for a number of sites, using a 4-year averaging period. The third case uses the lower value of 1.50 ± 0.15 ppmv y^{-1}, similar to the global estimate plotted by Tans et al.

Table 6. *Estimated atmospheric CO_2 budget (in Gt C y^{-1}) for 1986–1987, fitting CO_2 and $^{13}CO_2$ data to estimate relative regional contributions of the terrestrial components*

Component	Unconstrained ocean	Constrained ocean	Low CO_2 trend
fossil	5.24 ± 0.29	5.23 ± 0.29	5.24 ± 0.29
CO	0.89 ± 0.20	0.90 ± 0.20	0.89 ± 0.20
Biotic uptake			
tropical America	-2.24 ± 1.14	-1.98 ± 1.11	-2.24 ± 1.14
tropical Africa	-1.42 ± 1.25	-1.16 ± 1.23	-1.41 ± 1.25
tropical Asia	0.30 ± 1.25	0.49 ± 1.24	0.30 ± 1.25
evergreen	0.70 ± 1.08	0.91 ± 1.07	0.70 ± 1.08
deciduous	-1.95 ± 0.93	-1.98 ± 0.93	-1.95 ± 0.93
boreal	1.38 ± 0.69	1.33 ± 0.69	1.37 ± 0.69
grassland	-0.67 ± 1.36	-0.51 ± 1.35	-0.68 ± 1.36
other	0.21 ± 0.98	0.27 ± 0.97	0.18 ± 0.98
Land-use			
America	0.34 ± 0.49	0.37 ± 0.49	0.34 ± 0.49
Africa	0.25 ± 0.49	0.28 ± 0.49	0.25 ± 0.49
Asia	0.60 ± 0.49	0.64 ± 0.49	0.60 ± 0.49
other	0.26 ± 0.30	0.26 ± 0.30	0.25 ± 0.30
Oceans			
far north Atlantic	-1.20 ± 0.30	-1.22 ± 0.30	-1.23 ± 0.30
far north Pacific	0.11 ± 0.21	0.09 ± 0.21	0.10 ± 0.21
north Atlantic	-0.02 ± 0.38	-0.15 ± 0.37	-0.08 ± 0.38
north Pacific	-0.69 ± 0.46	-0.83 ± 0.44	-0.76 ± 0.46
equatorial west Pacific	1.29 ± 0.67	1.16 ± 0.66	1.25 ± 0.67
equatorial east Pacific	0.69 ± 0.71	0.55 ± 0.69	0.65 ± 0.71
equatorial Atlantic	0.26 ± 0.64	0.08 ± 0.62	0.23 ± 0.64
equatorial Indian	0.92 ± 0.58	0.79 ± 0.57	0.87 ± 0.58
south Atlantic	-0.02 ± 0.87	-0.10 ± 0.87	-0.07 ± 0.87
south Pacific	-1.49 ± 1.09	-1.63 ± 1.08	-1.59 ± 1.09
south Indian	-0.59 ± 0.78	-0.68 ± 0.78	-0.63 ± 0.78
southern	0.65 ± 0.46	0.64 ± 0.46	0.61 ± 0.46
net ocean	-0.07 ± 1.16	-1.32 ± 0.29	-0.66 ± 1.16
net biota	-2.24 ± 1.18	-1.08 ± 0.54	-2.28 ± 1.18

The "unconstrained ocean" is the standard case, the "constrained ocean" case modifies this by imposing a -1.4 ± 0.3 Gt C y^{-1} constraint on the net ocean flux. The "low CO_2 trend" case removes the ocean constraint but uses a growth rate of 1.5 ± 0.15 ppmv y^{-1} instead of 1.8 ± 0.15 ppmv y^{-1}.

(1991) which suggested that our running means may have given over-estimates because of the large growth in 1988. The results for the three cases are:

(i) The standard fit to the data sets described above. This case can be regarded as generalising the analysis of Enting et al. (1993) by a greater degree of disaggregation. As in many of the cases presented by Enting et al., the small net air-sea flux is comparable to that calculated by Tans et al. (1993). The reason for this is that in the inversion, the net air-sea flux is determined by the joint global budgets of CO_2 and $^{13}CO_2$. Since our analysis is essentially equivalent to that of Tans et al. (1993) using the same ocean $\delta^{13}C$ data, but differing slightly in the disequilibrium of the terrestrial biota, the results can be expected to be similar.

(ii) Since these low ocean uptake values contradict estimates from ocean modelling (e.g., Siegenthaler and Sarmiento, 1993) and also the estimate based on ocean ^{13}C inventories from Quay et al. (1992), we have produced our second estimate by using an additional constraint of -1.4 ± 0.3 Gt C y^{-1} on the net sea-air CO_2 flux. (After including transport of carbon via rivers, this equates to a net rate of increase of ocean carbon of 2.0 ± 0.3 Gt C y^{-1}). The constraint from ocean carbon modelling represents the imposition of a decadal time scale on the solution because ocean models do not reflect smaller-scale variations. Similarly the Quay et al. (1992) budget estimate based on ocean ^{13}C inventories was a 20-year average. Given the relative constancy in the spatial gradient of CO_2 over 1980–1987, we believe that the imposition of such a decadal constraint is reasonable. The results are shown in the second column of Table 6. Fig. 1 shows the zonal means of the mean components of the solution for CO_2 fluxes. Fig. 2 shows the main components of the isotopic anomaly flux. The use of such long-term constraints is similar to the use of the box-diffusion model by Keeling et al. (1989b) to prescribe the global budget. However this type of approach means that we are not achieving the ideal of a short-term "snapshot" of the carbon budget.

(iii) As a third case (suggested by the trend estimates by Tans (1991) and the results for the 1989–1990 inversion), we have removed the constaint on the total ocean and used a lower value

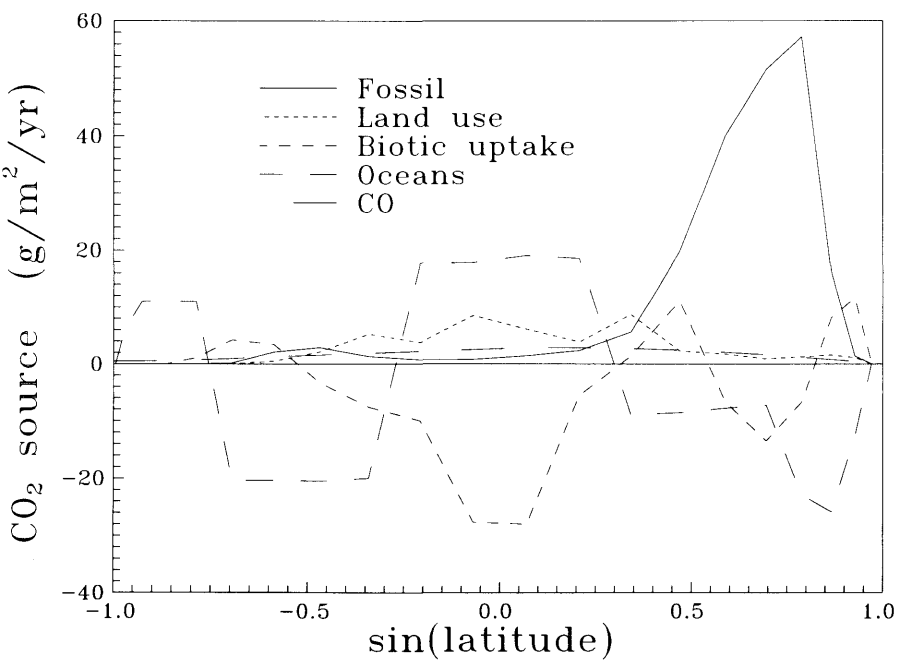

Fig. 1. Main components of zonal mean CO_2 fluxes for 1986–1987 ("constrained ocean" case from Table 6).

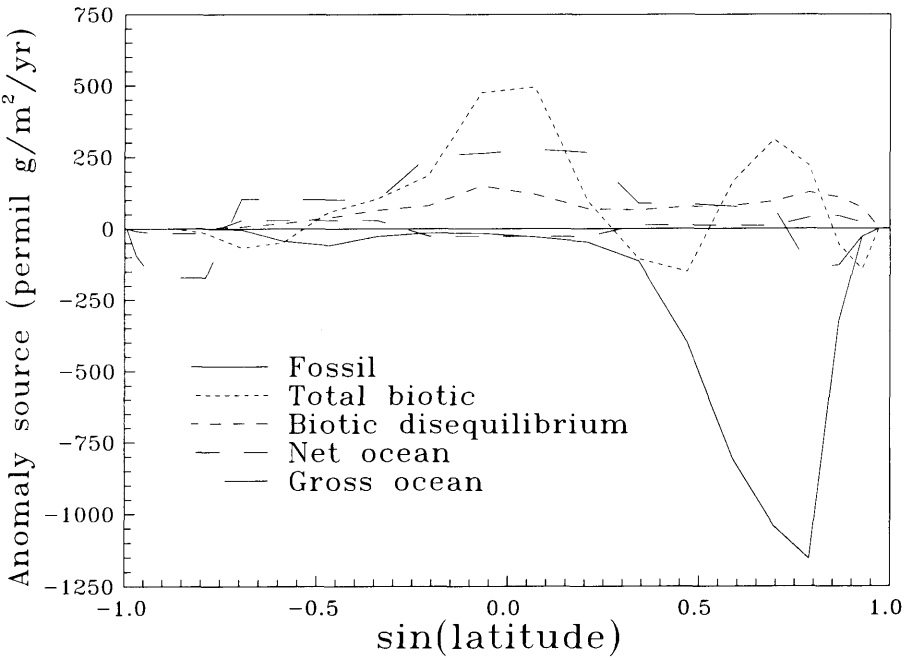

Fig. 2. Main components of zonal mean anomaly fluxes, 1986–1987 ("constrained ocean" case from Table 6).

of the global CO_2 trend: 1.50 ± 0.15 ppmv y^{-1}. With this lower growth rate, the global $CO_2/^{13}C$ balance implies larger ocean carbon uptake. The solution is the final column of Table 6 and has been considered in more detail by Enting (1995).

A key result of our studies is, as indicated in Figs. 4 and 5, that the constraints from spatial distributions of CO_2 determine the relative contributions from various regions but that these constraints are not sufficiently tight to provide useful new information about the global budget. The main constraints on the global budget come from the joint balance of global rates of change of CO_2 and ^{13}C. The results in Table 6 illustrate this: quite different results are obtained for the relative contributions of oceanic and terrestrial sinks, but these are achieved with relatively small shifts in regional fluxes. Figs. 3 and 4 show the zonal mean sources for oceanic and biotic components for the constrained and unconstrained cases, again illustrating the similarity in the distributions.

Enting (1995) presented a complementary analysis in terms of uncertainties in global ocean uptake, by using various subsets of the data set used for the unconstrained, low-trend, case (i.e., the final column of Table 6 in this paper). He began by using only the prior estimates plus the CO_2 trend. This led to a standard deviation of 2.20 in $\hat{S}_N$, the estimated net air-sea CO_2 flux. From this base case, he showed that adding the ^{13}C trend reduced the uncertainty in the net oceanic sink (1.40 s.d. in $\hat{S}_N$) with little reduction in the uncertainties of regional contributions, while using the spatial distributions of CO_2 (without the ^{13}C data) reduced the uncertainties in regional contributions but gave little improvement for the global budget (2.13 s.d. in $\hat{S}_N$). Combining spatial distributions with CO_2 and ^{13}C trends gave a global budget only slightly more precise (1.20 s.d. in $\hat{S}_N$) than that obtained from only the CO_2 and ^{13}C trends. Adding the spatial distribution of ^{13}C (corresponding to the final column of Table 6) gave little further improvement (1.16 s.d. in $\hat{S}_N$).

Key features of the spatial distribution apparent in each of the cases in Table 6 are:

- The inversions require an oceanic CO_2 source in the region south of 48° S.
- The terrestrial biotic fluxes in the northern

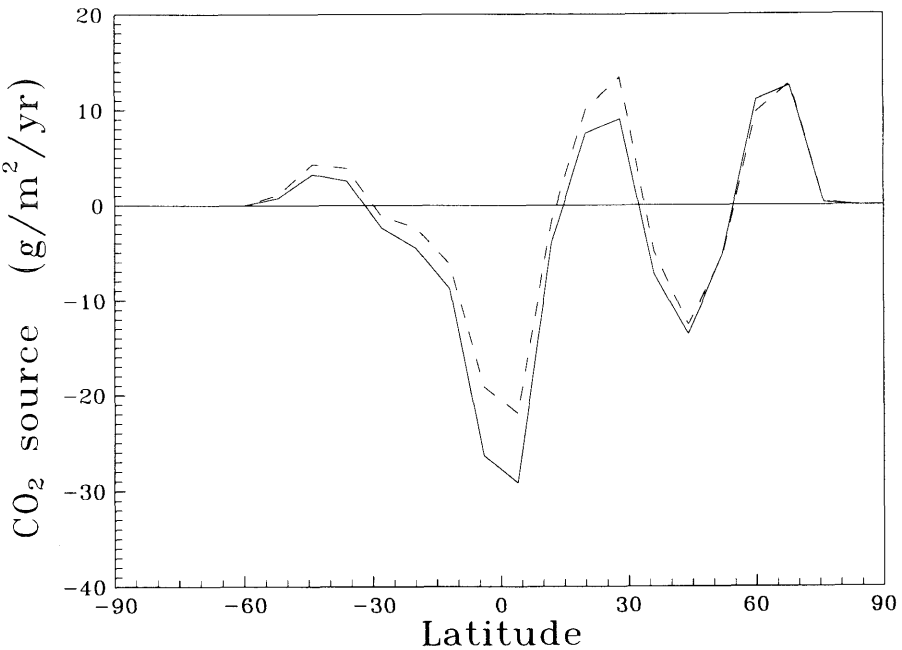

Fig. 3. Zonal means of oceanic CO_2 sources for 1986–1987 "unconstrained ocean" (solid) and "constrained ocean" (dashed) cases from Table 6.

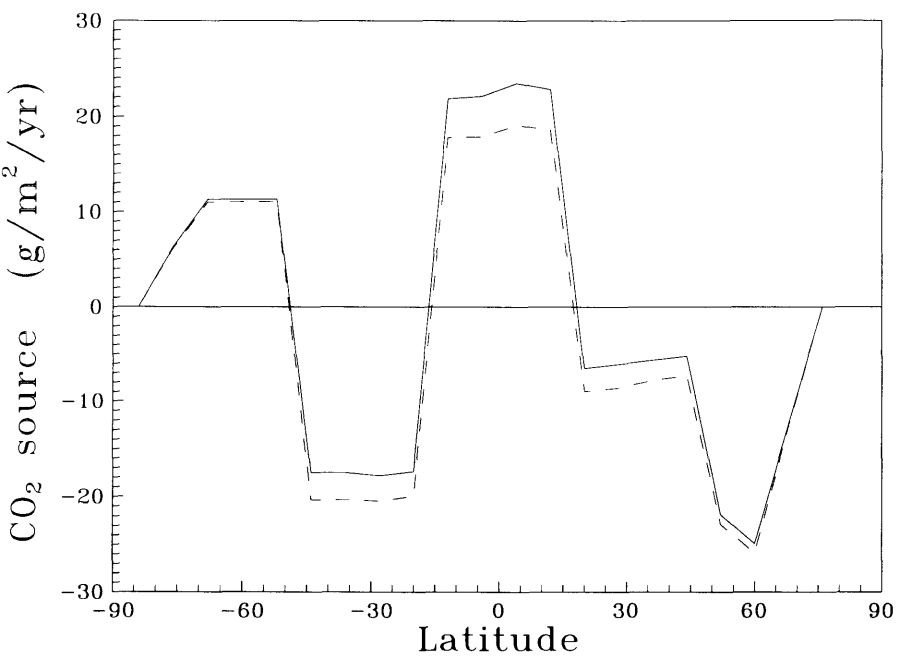

Fig. 4. Zonal means of terrestrial (non-fossil) sources. Cases as for Fig. 3.

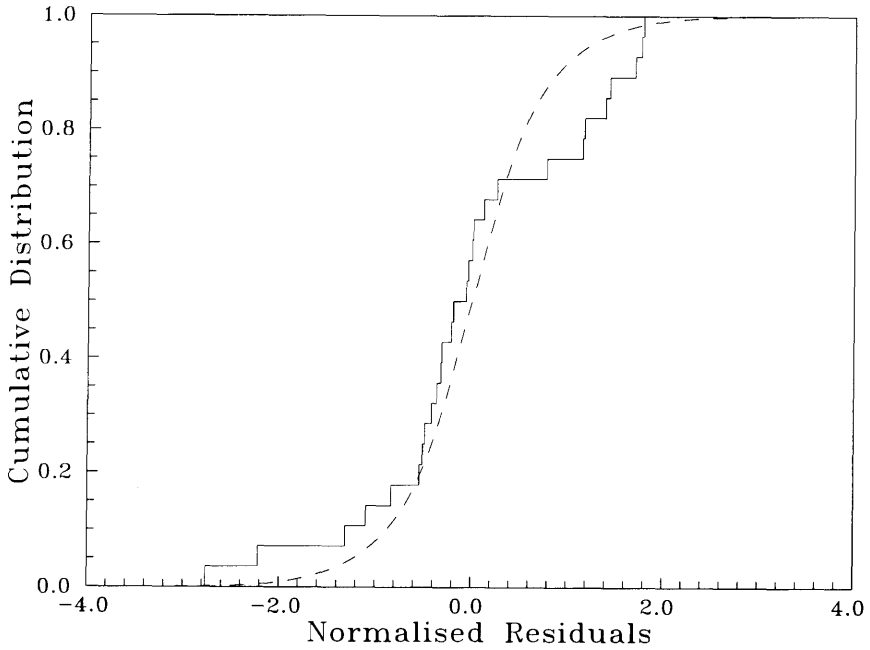

Fig. 5. Cumulative distribution of normalised residuals for the "unconstrained ocean 1986–1987" case from Table 6 (solid line) and the cumulative normal distribution (dashed curve).

hemisphere have a source in boreal forests balanced by a sink in deciduous forests. This feature appears to be necessary to reproduce the spatial gradients of $\delta^{13}C$.

• The source strengths in the equatorial Pacific were strong in the west and weak in the east, i.e., the opposite to what would be expected on the basis of the p_{CO_2} data presented by Tans et al. (1990a) and Murphy et al. (1991). However, the weaker eastern source is consistent with reduced upwelling due to the El Niño conditions in this period.

• The estimated "uptake" term for Asia is positive, implying a source rather than a sink. Since the inversion partitions biotic fluxes into "uptake" and "land-use" solely on the basis of the temporal behaviour, the positive "uptake" most probably reflects an inadequacy in our representation of the seasonality of one or both components. Alternatively it could be a bias due to errors in other aspects of the seasonality, either in sources or atmospheric transport. However the apparent source could also reflect a real effect associated with El-Niño/Southern Oscillation variations, given the correlation between the SOI and southeast Asian precipitation (see for example, Keeling et al., 1989a, p. 207).

• The seasonal cycle strengths (NPPs of 43 Gt C y^{-1} in each case) are closer to the prior estimate in these disaggregated cases than in the aggregated inversion presented by Enting et al. (1993).

5.2. *The period 1989–1990*

Over the period 1989–1991, the $\delta^{13}C$ of atmospheric CO_2 showed a dramatic change in behaviour relative to the earlier direct measurements and the majority of ice-core records. The long-term decrease ($\approx -0.03^{o}/_{oo}\,y^{-1}$) stopped and was replaced by a period of near-constant or slightly increasing $\delta^{13}C$. This phenomenon was global in extent and has been found by several different global ^{13}C programs (Francey et al., 1995).

Other carbon cycle changes that occured at about this time were as follows.

• The pole-to-pole difference in CO_2 concentration increased from being 3 ppmv over most of the period 1980–1987, to 4 ppmv post-1988.

• The global growth rate of atmospheric CO_2 showed large variations (Tans, 1991).

• The amplitude of the seasonal cycle at several northern sites increased after being relatively constant over most of the 1980's (Whorf and Keeling, 1991).

• We also note that during the early part of the 1980's the steady increase in fossil emission rates ceased for several years, but the resumption in growth was several years before the other anomalies.

The inversion techniques used here are designed for quasi-steady state situations and so can not be expected to be reliable in the transient situations that applied over the period 1988–1991. Nevertheless, the abnormality in the $\delta^{13}C$ record makes it of considerable interest to try to interpret the data for this period. We have therefore chosen 1989–1990 as our reference period and applied the inversion technique using the CO_2 and ^{13}C data from the relevant columns of Tables 4, 5. We use a global trend of 1.5 ± 0.5 to reflect the greater uncertainty. The results are tabulated in Table 7.

We repeated the inversion for 1989–1990 with the data from the NOAA shipboard sampling program removed. The reason for this is that the inversion with all data had Samoa with a 0.87 ppmv residual for 1989–1990, compared to 0.36 ppmv for the 1986–1987 calculations for which no ship data were available. Studies by Enting (1993) had indicated that much of the uncertainty in estimates of southern sources could arise because of the large latitudinal gap between Samoa and Cape Grim. With the ship data excluded, the residual for Samoa changed from 0.87 to 0.25 ppmv and the character of the solution changed dramatically.

Key features of the solutions are as follows:

• The two cases for 1989–1990 differ more than any of the cases for the 1986–1987 inversion (see Subsection 5.1 and Enting et al., 1993). The differences occur mainly in the southern hemisphere and to a lesser extent in equatorial regions. There appears to be a genuine discrepancy. This may reflect problems with the ship-based data. More plausibly, the instability may be due to the spatial distribution being inconsistent with the assumption of a quasi-steady state, given the abrupt changes listed above.

• Ocean sinks, 1.67 and 1.78 Gt C y^{-1} are obtained without the imposition of any additional constraints. Examination of the fits shows that these solutions are being achieved by predicting low CO_2 trends (1.21 and 1.14 ppmv y^{-1}) and an increase in the isotopic disequilibrium relative to 1986–1987.

• In each case, the eastern Pacific is a stronger source than the western Pacific, as expected from p_{CO_2} data but unlike the solutions for 1986–1987. The La Niña conditions in this period would suggest a stronger than "normal" source from eastern Pacific upwelling.

Table 7. *Estimated atmospheric CO_2 budget (in Gt C y^{-1}) for 1989–1990, fitting CO_2 and $^{13}CO_2$ data to estimate relative regional contributions of the terrestrial components*

Component	Estimate all data	Estimate no ship data
fossil	5.65 ± 0.29	5.66 ± 0.30
CO	0.87 ± 0.20	0.87 ± 0.20
Biotic uptake		
tropical America	0.42 ± 1.15	-0.26 ± 1.18
tropical africa	-1.58 ± 1.26	-1.43 ± 1.26
tropical Asia	-2.04 ± 1.25	-1.57 ± 1.26
evergreen	-0.54 ± 1.12	-0.50 ± 1.16
deciduous	-1.44 ± 0.96	-1.36 ± 0.96
boreal	1.45 ± 0.71	1.39 ± 0.72
grassland	-0.82 ± 1.36	-0.84 ± 1.36
other	1.00 ± 0.98	$0.99 + 0.98$
Land-use		
America	0.55 ± 0.49	0.46 ± 0.49
Africa	0.13 ± 0.49	0.16 ± 0.49
Asia	0.37 ± 0.49	0.41 ± 0.49
other	0.22 ± 0.30	0.23 ± 0.30
Oceans		
far north Atlantic	-1.08 ± 0.33	-1.09 ± 0.33
far north Pacific	0.05 ± 0.21	0.00 ± 0.22
north Atlantic	-1.27 ± 0.44	-1.18 ± 0.45
north Pacific	-0.75 ± 0.39	-0.56 ± 0.48
equatorial west Pacific	0.40 ± 0.52	0.90 ± 0.67
equatorial east Pacific	1.97 ± 0.55	1.23 ± 0.72
equatorial Atlantic	0.82 ± 0.61	0.96 ± 0.61
equatorial Indian	0.47 ± 0.59	0.67 ± 0.59
south Atlantic	-1.13 ± 0.85	-0.93 ± 0.86
south Pacific	0.16 ± 0.61	-1.50 ± 1.10
south Indian	-1.32 ± 0.77	-0.94 ± 0.79
southern	-0.01 ± 0.37	0.65 ± 0.46
net ocean	-1.67 ± 1.51	-1.78 ± 1.51
net biota	-2.27 ± 1.27	-2.32 ± 1.27

• As might be expected, the inclusion of the ship data reduces the uncertainties most for the Pacific regions, particularly in the equatorial and southern mid-latitude regions.

6. Error calculations

Enting (1995) noted three ways in which one could obtain estimates of the errors in the solutions of sets of equations such as (1). These were as follows.

(i) Track the uncertainties in the data through the inversion of (1) using prior uncertainty estimates derived from characteristics of the data records.

(ii) Track the uncertainties in the data through the inversion of (1) using uncertainty estimates based on the distribution of residuals to the fit to eq. (1).

(iii) Assess the uncertainty in the solution from the extent to which the solution is sensitive to the choice of data set.

Approach (i) is used in all the calculations presented here. In terms of approach (iii), Enting et al. (1993) noted that the ocean uptake estimates that they obtained for various cases suggested that the range of about ± 1 Gt C y^{-1} obtained from approach (i) was realistic, and this applies equally well to the ± 1.16 Gt C y^{-1} obtained here. In order to explore the consistency of (i) and (ii) we have calculated the variance of the residuals (normalised by the data uncertainties) for the "unconstrained 1986–1987" solution (from Table 6) as 1.22. For further comparison, Fig. 5 plots the cumulative distribution of these normalised residuals compared to the cumulative normal distribution. The agreement gives additional confirmation that our prior estimates of the uncertainties in the data are realistic.

The capability of assessing the uncertainties in the inversions of atmospheric CO_2 data represents an important improvement over earlier inversion formalisms. The uncertainty analysis is, of course, of direct interest in evaluating how well we understand the global carbon cycle with all the implications that follow regarding the predictability of future CO_2 levels. However, the ability to assess the uncertainties in the estimated budget gives us a tool that allows for quantitative comparisons between alternative measures that are proposed for reducing uncertainties. For example, we can compare the relative utility of adding additional measurement sites as opposed to refining the precision at existing sites. It is a characteristic of least-squares solutions that the covariances of the estimates depend on the covariances of the data but not on the values of the data items. This makes it possible to explore the consequences of hypothetical improvements in data quality without having actual results. This can be extended to the more general problem of designing sampling networks to optimise the detectability of particular source components. It is also possible to assess the utility of improvements in direct estimates, those that form the "priors" in our estimation procedure. Improvements in our knowledge of any one component will translate to a reduction of uncertainty in all other components. Our formalism provides a tool for determining when such improvements are large enough to be useful.

As a particular example, we have repeated the calculations for the "unconstrained 1986–1987" case with a precision of 0.1 ppmv for the annual means of CO_2 in place of the 0.3 ppmv used in the standard cases. The result is that the uncertainty in the net ocean uptake decreased from ± 1.16 to ± 1.11 Gt C y^{-1}. This provides additional confirmation of our result that the division of the global total into oceanic and biotic components is constrained primarily by the trends in CO_2 and $\delta^{13}C$, neither of which was changed in this test case. The hypothetical three-fold improvement in network precision gives most improvement outside the tropics, with 20% to 50% reductions in the uncertainties for ocean fluxes and similar reductions for the "deciduous" and "boreal" biotic uptakes. Smaller reductions in uncertainty (10% to 20%) are achieved for tropical ocean fluxes. Virtually no improvement is obtained for the components of the tropical biota because of the ambiguity between the uptake and land-use components.

7. Conclusions

From the results of the inversions presented here (and from Enting et al., 1993; Enting, 1995), it is clear that on a global scale, the relative roles of the oceans and biota as sinks of anthropogenic CO_2 are determined primarily by the atmospheric CO_2

Tellus B/47/1/2-4

and $^{13}CO_2$ trends. The spatial distributions play a lesser role in constraining the relative contributions of oceanic and terrestrial sources and sinks. Essentially the same conclusion resulted from the analysis by Enting (1992) using a regional decomposition (as opposed to a process-based decomposition) incorporating inversion results from two-dimensional modelling.

Our posterior estimates of the uncertainties in the sources are derived from a priori estimates of the uncertainty in the data. Simple assessments using alternative approaches to error estimation confirm that our values for uncertainties are realistic. The ability to quantify the uncertainties provides a powerful new tool for interpreting CO_2 data. By quantifying the uncertainties, and finding them to be large, we can appreciate how various different approaches to quantifying the carbon budget have arrived at apparently inconsistent conclusions.

The precision to which the atmospheric carbon budget can be determined on the global scale will depend critically on the precision with which the atmospheric $^{13}CO_2$ budget can be established. Progress in this area will require better spatial coverage and a more precise knowledge of the isotopic disequilibrium effects of the biota and more importantly, the oceans.

8. Acknowledgments

The atmospheric transport model was kindly provided by I. Y. Fung of NASA Goddard Institute of Space Sciences and implemented at CSIRO by J. V. Mansbridge. The DAR stable isotope program has relied heavily on the staff of GASLAB at DAR and CGBAPS. The Cheeka Peak data were kindly supplied by P. D. Quay. H. Granek assisted with the statistical analysis. G. I. Pearman, A. J. Hirst and an anonymous referee provided useful comments on the manuscript. Suggestions from S. Piper for clarification were particularly valuable. The authors wish to thank P. P. Tans for supplying a copy of his 1993 paper prior to publication, G. Marland for supplying the fossil ^{13}C data, I. Y. Fung for stimulating discussions. The CSIRO transport modelling project was funded by the State Electricity Commission of Victoria.

9. Appendix A

Units and normalisations

- The observed CO_2 data are expressed in ppmv (parts per million by volume), except for the trend terms which are in ppmv per year.
- The $^{13}CO_2$ data are expressed as a ^{13}C anomaly, X, as defined in Subsection 2.2, with units of $^{o}/_{oo}$ ppmv.
- The pseudo-sources defining global mean concentrations are expressed in the units of the corresponding concentrations, for convenience.
- Real sources, σ_μ, are in Gt C y^{-1} (gigatonnes of carbon per year); in most cases this is the annual mean source strength, the exception being the seasonal cycle where the σ_μ denotes the NPP. We choose the sign convention that sources to the atmosphere are positive.
- The gross fluxes between atmosphere and biota and atmosphere and oceans are expressed as Gt C y^{-1} for consistency, even though the gross flux terms do not appear in the carbon budget, being required only in calculating the effect of isotopic disequilibrium.

10. Appendix B

Notation

a	area of an ocean region.
$c_j \pm u_j$	jth item of observational data and its s.d.
L	number of constraints in addition to observed concentrations and prior source estimates.
M	number of observations fitted.
N	number of real source components.
N'	number of source components estimated—includes "pseudo-sources".
$q_{\alpha\mu}$	factor defining linear combination of source components—the amount of the μth source in the αth combination, x_α.
R_a	atmospheric ^{13}C:C ratio $(= {}^{13}C/({}^{12}C + {}^{13}C))$.
R_m	mixed layer ^{13}C:C ratio.
R_{ref}	reference ^{13}C:C ratio used for defining isotopic anomalies.
$s_\mu \pm v_\mu$	prior estimate for σ_μ, with s.d.
S_G	isotopic anomaly flux due to isotopic disequilibrium.
S_N	net air-sea carbon flux $= \Phi_{am} - \Phi_{ma}$.

S^*	net sea-air ^{13}C flux $= \alpha_{am} R_a \Phi_{am} - \alpha_{ma} R_m \Phi_{ma}$.	α_{am}	kinetic air-sea ^{13}C:C fractionation factor (the numerical values are taken from ^{13}C:^{12}C fractionation factors because the differences are negligible in the present context).
S_X	net sea-air ^{13}C anomaly flux $= S_G + S_N(\alpha_{am} R_a / R_r - 1) \times 1000$.		
t	time (years).		
$t_\beta \pm r_\beta$	value of βth additional constraint, with s.d.	α_{ma}	kinetic sea-air ^{13}C:C fractionation factor.
$T_{j\mu}$	contribution to observation j from source μ.	κ	air-sea gas exchange coefficient for CO_2, in g m^{-2} y^{-1} μatm^{-1}.
$V_{\mu\eta}$	covariance of the estimates $\hat{\sigma}_\mu$ and $\hat{\sigma}_\eta$.	μ	general index for source components.
x_α	linear combination of source components, σ_μ.	$\sigma_\mu, \hat{\sigma}_\mu$	μth source component and its estimated value.
X	isotopic anomaly. $X = ([^{13}C]/R_{ref} - [C]) \times 1000$.	Φ_{am}, Φ_{ma}	gross CO_2 fluxes, air-to-sea and sea-to-air.

REFERENCES

Andres, R. J., Marland, G., Boden, T. and Bischoff, S. 1995. Carbon dioxide emissions from fossil fuel combustion and cement manufacture 1751–1991 and an estimate of their isotopic composition and latitudinal distribution. In: *The carbon cycle*, ed. T. M. L. Wigley (Cambridge University Press, Stanford), in press.

Azevedo, A. E. 1982. *Atmospheric distribution of CO_2 and its exchange with the biosphere and the oceans.* PhD Thesis, Columbia University, New York.

CDIAC 1991. *Trends 91: A compendium of data on global change*, ed. T. A. Boden, R. J. Serpanski and F. W. Stoss (Carbon dioxide information Analysis Center: Oak Ridge).

CMDL 1992: *Climate monitoring and diagnostics laboratory*, no. 20, Summary Report 1991, ed. E. E. Ferguson and R. M. Rosson (US Dept. Commerce: Washington).

Emanuel, W. R., Killough, G. E. G. and Olson, J. S. 1981. Modelling the circulation of carbon in the world's terrestrial ecosystems, pp. 335–364 of *Carbon cycle modelling*. SCOPE 16, ed. B. Bolin (Wiley: Chichester).

Enting, I. G. 1992. *Constraining the atmospheric carbon budget: a preliminary assessment.* Division of Atmospheric Research Technical Paper No. 25: (CSIRO, Australia).

Enting, I. G. 1993. Inverse problems in atmospheric constituent studies. III: Estimating errors in surface sources. *Inverse Problems* **9**, 649–665.

Enting, I. G. 1995. Constraints on the atmospheric carbon budget from spatial distributions of CO_2. In: *The carbon cycle*, ed. T. M. L. Wigley (Cambridge University Press, Stanford), in press.

Enting, I. G. and Mansbridge, J. V. 1991. Latitudinal distribution of sources and sinks of CO_2: Results of an inversion study. *Tellus* **43B**, 156–170.

Enting, I. G. and Newsman, G. N. 1990. Inverse problems in atmospheric constituent studies: II. Sources in the free atmosphere. *Inverse Problems* **6**, 349–362.

Enting, I. G. and Pearman, G. I. 1987. Description of a one-dimensional carbon cycle model calibrated using techniques of constrained inversion. *Tellus* **39B**, 459–476.

Enting, I. G., Trudinger, C. M., Francey, R. J. and Granek, H. 1993. *Synthesis inversion of atmospheric CO_2 using the GISS tracer transport model.* Division of Atmospheric Research Technical Paper No. 29. (CSIRO, Australia).

Francey, R. J. and Goodman, H. S. 1986. Systematic error in, and selection of, in situ $\delta^{13}C$. *Baseline atmospheric program* (Australia) 1983–1984, eds. R. J. Francey and B. W. Forgan (Department of Science, Bureau of Meteorology/CSIRO, Division of Atmospheric Research: Australia), pp. 27–36.

Francey, R. J. and Goodman, H. S. 1988. The DAR stable isotope reference scale for CO_2. *Baseline atmospheric program* (Australia) 1986, ed. B. W. Forgan and P. J. Fraser (Department of Science and CSIRO: Australia), pp. 40–46.

Francey, R. J., Robbins, F. J., Allison, C. E. and Richards, N. G. 1990. The CSIRO global survey of CO_2 stable isotopes. *Baseline atmospheric program* (Australia) 1988, ed. S. R. Wilson and G. P. Ayers (Dept. of Admin. Services and CSIRO: Australia), pp. 16–27.

Francey, R. J., Allison, C. E., Enting, I. G., White, J., Trolier, M. and Tans, P. P. 1995. The trend in atmospheric $\delta^{13}C$, *Nature*, in press.

Friedli, H., Lötscher, H., Oeschger, H., Siegenthaler, U. and Stauffer, B. 1986. Ice core record of the $^{13}C/^{12}C$ ratio of atmospheric CO_2 in the past two centuries. *Nature* **324**, 237–238.

Fung, I., Prentice, K., Matthews, E., Lerner, J. and Russell, G. 1983. Three-dimensional tracer model study of atmospheric CO_2: response to seasonal exchanges with the terrestrial biosphere. *J. Geophys. Res.* **88C**, 1281–1294.

Fung, I., John, J., Lerner, J., Matthews, E., Prather, M., Steele, L. P. and Fraser, P. J. 1991. Three-dimensional model synthesis of the global methane cycle. *J. Geophys. Res.* **96D**, 13033–13065.

GMCC 1988. *Geophysical monitoring for climatic change*, No. 16. Summary Report 1987, ed. B. Bodhaine and R. M. Rosson (US Dept. Commerce: Washington).

Heimann, M. and Keeling, C. D. 1989. A three-dimensional model of atmospheric CO_2 transport based on observed winds: 2. Model description and simulated tracer experiments. *Aspects of climate variability in the Pacific and western Americas.* Geophysical Monograph **55**, ed. D. H. Peterson. (AGU: Washington).

Houghton, R. A., Boone, R. D., Fruci, J. R., Hobbie, J. E., Melillo, J. M., Palm, C. A., Peterson, B. J., Shaver, G. R., Woodwell, G. M., Moore, B., Skole, D. L. and Myers, N. 1987. The flux of carbon from terrestrial ecosystems to the atmosphere in 1980 due to changes in land use: geographic distribution of the global flux. *Tellus* **39B**, 122–139.

Keeling, C. D., Bacastow, R. B., Carter, A. F., Piper, S. C., Whorf, T. P., Heimann, M., Mook, W. G. and Roeloffzen, H. 1989a. A three-dimensional model of atmospheric CO_2 transport based on observed winds: (1). Analysis of observational data. *Aspects of climate variability in the Pacific and western Americas.* Geophysical Monograph **55**, ed. D. H. Peterson (AGU: Washington).

Keeling, C. D., Piper, S. C. and Heimann, M. 1989b. A three-dimensional model of atmospheric CO_2 transport based on observed winds: 4. Mean annual gradients and interannual variations. *Aspects of climate variability in the Pacific and western Americas.* Geophysical Monograph **55**, ed. D. H. Peterson (AGU: Washington).

Marland, G., Rotty, R. M. and Treat, N. L. 1985. CO_2 from fossil fuel burning: Global distribution of emissions. *Tellus* **37B**, 243–258.

Matthews, E. 1985. *Atlas of archived vegetation land-use and seasonal albedo data sets.* NASA Technical Memorandum no. 86199.

Murphy, P. P., Feely, R. A., Gammon, R. H., Harrison, D. E., Kelly, K. C. and Waterman, L. S. 1991. Assessment of the air-sea exchange of CO_2 in the South Pacific during Austral autumn. *J. Geophys. Res.* **96C**, 20455–20465.

Newsam, G. N. and Enting, I. G. 1988. Inverse problems in atmospheric constituent studies: I. Determination of surface sources under a diffusive transport approximation. *Inverse Problems* **4**, 1037–1054.

Pearman, G. I. and Hyson, P. 1986. Global transport and inter-reservoir exchange of carbon dioxide with particular reference to stable isotope distribution. *J. Atmos. Chem.* **4**, 81–124.

Prather, M., McElroy, M., Wofsy, S., Russell, G. and Rind, D. 1987. Chemistry of the global troposphere: Fluorocarbons as tracers of air motion. *J. Geophys. Res.* **92**, 6579–6613.

Press, W. H., Flannery, B. P., Teukolsky, S. A. and Vetterling, W. T. 1986. *Numerical recipes: the art of scientific computing* (Cambridge University Press).

Prinn, R., Cunnold, D., Rasmussen, R., Simmonds, P., Alyea, F., Crawford, A., Fraser, P. and Rosen, R. 1987. Atmospheric trends in methyl chloroform and the global average for the hydroxyl radical. *Science* **238**, 945–950.

Quay, P. D., Tilbrook, B. and Wong, C. S. 1992. Oceanic uptake of fossil fuel CO_2: Carbon-13 evidence. *Science* **256**, 74–79.

Rotty, R. M. 1987. Estimates of seasonal variation in fossil fuel CO_2 emissions. *Tellus* **39B**, 184–202.

Russell, G. and Lerner, J. 1981. A new finite differencing scheme for the tracer transport equation. *J. Appl. Meteorol.* **20**, 1483–1498.

Sarmiento, J. L. and Sundquist, E. T. 1992. Revised budget for the oceanic uptake of anthropogenic carbon dioxide. *Nature* **356**, 589–593.

Siegenthaler, U. and Sarmiento, J. L. 1993. Atmospheric carbon dioxide and the ocean. *Nature* **356**, 119–125.

Tans, P. P. 1981. $^{13}C/^{12}C$ of industrial CO_2, pp. 127–129 of *Carbon cycle modelling. SCOPE 16*, ed. B. Bolin (Wiley: Chichester).

Tans, P. P., Fung, I. Y. and Takahashi, T. 1990a. Observational constraints on the global atmospheric CO_2 budget. *Science* **247**, 1431–1438.

Tans, P. P., Thoning, K. W., Elliott, W. P. and Conway, T. J. 1990b. Error estimates of background atmospheric CO_2 patterns from weekly flask samples. *J. Geophys. Res.* **95D**, 14063–14070.

Tans, P. P. (Ed). 1991. Carbon cycle group, ch. 4, pp. 24–33 of *Climate monitoring and diagnostics laboratory*, no. 19. Summary Report 1990, ed. E. E. Ferguson and R. M. Rosson (US Dept. Commerce: Washington).

Tans, P. P., Berry, J. A. and Keeling, R. F. 1993. Oceanic $^{13}C/^{12}C$ observations: A new window on ocean CO_2 uptake. *Global Biogeochemical Cycles* **7**, 353–368.

Trenberth, K. E. 1981. Seasonal variations in global sea-level pressure and the total mass of the atmosphere. *J. Geophys. Res.* **86C**, 5238–5246.

Whorf, T. P. and Keeling, C. D. 1991. Seasonal amplitude variations of CO_2 in the northern hemisphere. *Climate monitoring and diagnostics laboratory*, no. 19. Summary Report 1990, ed. E. E. Ferguson and R. M. Rosson (US Dept. Commerce: Washington).

Wunsch, C. and Minster, J.-F. 1982. Methods for box models and ocean circulation tracers: mathematical programming and non-linear inverse theory. *J. Geophys. Res.* **87**, 5647–5662.